Fusion Engineering and Design xxx (2013) xxx–xxx

Contents lists available at SciVerse ScienceDirect

Fusion Engineering and Design

journal homepage: www.elsevier.com/locate/fusengdes

Nonlinear vacuum gas flow through a short tube due to pressure and temperature gradients

Sarantis Pantazis[a], Steryios Naris[a], Christos Tantos[a], Dimitris Valougeorgis[a,*], Julien André[b], Francois Millet[b], Jean Paul Perin[b]

[a] Department of Mechanical Engineering, University of Thessaly, Pedion Areos, 38334 Volos, Greece[1]
[b] Service des Basses Températures, UMR-E CEA/UJF-Grenoble 1, INAC, Grenoble, F-38054, France[2]

ARTICLE INFO

Article history:
Received 14 September 2012
Received in revised form 15 February 2013
Accepted 4 March 2013
Available online xxx

Keywords:
Vacuum gas dynamics
Knudsen
Kinetic theory
Pumping systems of DT fusion reactors

ABSTRACT

The flow of a rarefied gas through a tube due to both pressure and temperature gradients has been studied numerically. The main objective is to investigate the performance of a mechanical vacuum pump operating at low temperatures in order to increase the pumped mass flow rate. This type of pump is under development at CEA-Grenoble. The flow is modelled by the Shakhov kinetic model equation, which is solved by the discrete velocity method. Results are presented for certain geometry and flow parameters. Since according to the pump design the temperature driven flow is in the opposite direction than the main pressure driven flow, it has been found that for the operating pressure range studied here the net mass flow rate through the pump may be significantly reduced.

© 2013 Elsevier B.V. All rights reserved.

1. Introduction

The successful operation of DT fusion reactors requires the implementation of demanding vacuum systems capable of pumping large amounts of neutralized gases, helium and impurities. Operating the mechanical vacuum pumps at a lower temperature than the ambient one may be a solution to achieve large mass flow rates. This is easily seen by taking into consideration that at a given operating pressure the gas density is inversely proportional to its temperature. CEA-Grenoble has launched a long-term programme in that direction [1,2]. The cooling of the gas is taking place in a heat exchanger placed just before the mechanical pump.

It is well known however, that due to the wall temperature gradient of the heat exchanger a counter flow to the main pump flow is developed. This type of flow, known as thermal creep flow [3,4], is increased as the Knudsen number is increased and as a result the overall gain of operating in low temperatures may be significantly reduced. To investigate the effect of the thermal creep flow to the overall performance of the pump, the flow of a gas through the heat exchanger part of the cryo-mechanical-pump (CMP) is simulated.

Most of the previous work with combined pressure and temperature driven flows is focused on low-speed fully developed flows [2–6], while the corresponding work for high speed nonlinear flows is limited [7]. The work presented here is one of the first attempts to quantify the thermal creep phenomenon compared to the main pressure driven flow in the case of nonlinear flows.

2. Flow configuration

The heat exchanger, as shown in Fig. 1, is approximated as a vertical circular tube of diameter $D = 320$ mm and total length $L = 483$ mm ($L/D \simeq 1.5$). The tube wall temperature is 300 K at $x' = 0$ mm and 80 K at $x' = 295$ mm, while for the rest of the tube it remains constant at 80 K. The temperature drop from 300 K down to 80 K is assumed to be linear. The expected range of the inlet pressure varies significantly. Simulations have been carried out for helium, because it will be used in the experiments to be performed with the CMP prototype pump.

The main flow parameter is the Knudsen number or alternatively the gas rarefaction parameter, defined as

$$\delta = \frac{PD}{\mu \upsilon} \sim \frac{1}{Kn} \tag{1}$$

where P is the local pressure, while μ and υ are the viscocity and the most probable velocity at local temperature T. Based on the above conditions, the flow may be in a wide range of the Knudsen number and therefore a kinetic approach must be implemented. In this flow configuration there is a Poiseuille type flow due to the imposed pressure difference and a thermal creep type flow from the low towards the high wall temperature.

* Corresponding author. Tel.: +30 2421074058; fax: +30 2421074085.
E-mail address: diva@mie.uth.gr (D. Valougeorgis).
[1] Association EURATOM-Hellenic Republic.
[2] Association EURATOM-CEA.

0920-3796/$ – see front matter © 2013 Elsevier B.V. All rights reserved.
http://dx.doi.org/10.1016/j.fusengdes.2013.03.011

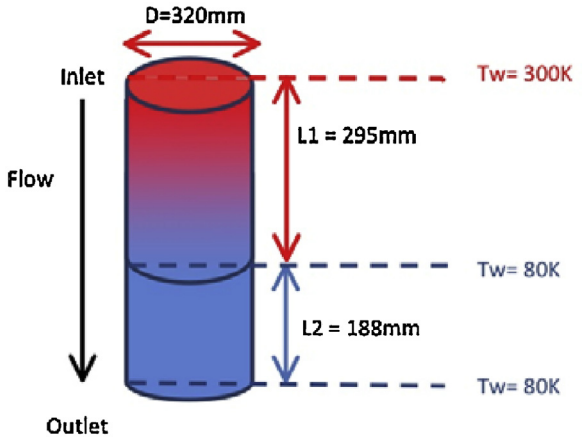

Fig. 1. Heat exchanger configuration.

The simulated flow configuration, shown in Fig. 2, consists of the tube with the above described geometric characteristics connecting two reservoirs A and B maintained at pressure and temperature (P_A, T_A) and (P_B, T_B) respectively. The two reservoirs correspond to the upstream dome and to the downstream baffle of the heat exchanger. The temperature of the tube wall is denoted by $T_W(x')$. The pressure and the temperature of the upstream reservoir are taken as reference quantities.

To investigate in detail the effect of the thermal creep flow on the overall flow the following four major cases are considered:

I. $P_A > P_B$, $T_A = T_W(x') = T_B = 300$ K
II. $P_A > P_B$, $T_A = T_W(x') = T_B = 80$ K
III. $P_A = P_B$, $T_A = 300$ K, $T_B = 80$ K, $300 \geq T_W(x') \geq 80$ K
IV. $P_A > P_B$, $T_A = 300$ K, $T_B = 80$ K, $300 \geq T_W(x') \geq 80$ K

Cases I and II correspond to purely pressure driven flow at two different reference temperatures. By comparing these results the advantages of operating in low temperatures will be demonstrated. Case III corresponds to the purely temperature driven flow with the tube wall temperature distribution applied here. It will provide the pure thermal creep flow rate. Finally, Case IV corresponds to the mixed flow conditions consisting of the pressure driven and the counter temperature driven flows. It is evident that considering each of these four major cases and comparing the obtained results will provide a clear estimation of the effect of the thermal creep flow on the overall flow. For each of the four cases (I–IV) two values of the reference pressure are considered: $P_A = 0.3$ and 0.03 Pa. The corresponding reference rarefaction parameters according to (1) are $\delta_A = 2.16$ and 0.216. Also, the downstream to upstream pressure ratio P_B/P_A is taken equal to 0.5 and 0.2. The flow parameters have been chosen such that a description of the flow characteristics in the transition regime $0.1 < \delta < 10$ is obtained.

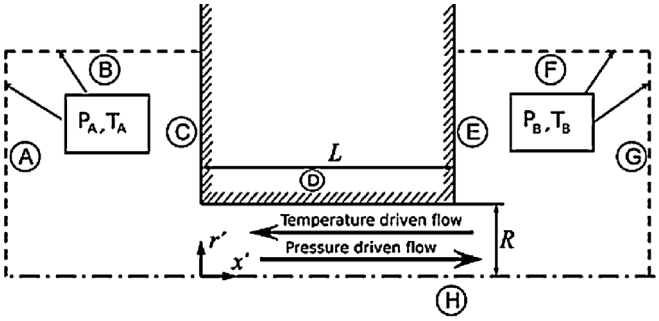

Fig. 2. Computational domain.

Table 1
Values of numerical parameters in the algorithm.

Numerical parameter	Value
Size of upstream and downstream reservoirs in unit lengths	15×15
Nodes per unit length	40
Number of discrete c_p	16
Number of discrete c_x	16
Number of polar angles θ	140
Convergence criterion imposed on the macroscopic quantities	10^{-7}

3. Kinetic formulation and numerical scheme

The governing kinetic model equation describing efficiently the flow is the Shakhov kinetic model equation [8] given by

$$c_p \cos\theta \frac{\partial g}{\partial r} - \frac{c_p \sin\theta}{r}\frac{\partial g}{\partial \theta} + c_x \frac{\partial g}{\partial x} = \delta_A \rho \sqrt{\tau}(g^S - g) \quad (2)$$

Here, $g = g(x, r, c_p, \theta, c_x)$ is the unknown distribution function with x and r denoting the axial and radial direction of the flow, while $\boldsymbol{c} = (c_p, \theta, c_x)$ is the molecular velocity in cylindrical coordinates. Also,

$$g^S = g^M \left[1 + \frac{4}{15\rho\tau^2} q \cdot (c-u)\left[\frac{(c-u)^2}{\tau} - \frac{5}{2}\right]\right]$$

with $g^M = [\rho/(\pi\tau)^{3/2}]\exp[-(\boldsymbol{c}-\boldsymbol{u})^2/\tau]$ denoting the local Maxwellian. Here, ρ, $\boldsymbol{u} = (u_x, u_r)$, τ and $\boldsymbol{q} = (q_x, q_r)$ denote the number density, velocity vector, temperature and heat flux vector respectively obtained by the corresponding moments of the unknown distribution function. All quantities are in dimensionless form with the tube radius R being the reference unit length and $\upsilon_A = \sqrt{2R_g T_A}$ the reference velocity ($R_g = 2065\ \mathrm{m^2/(s^2\ K)}$ is the gas constant).

The associated boundary conditions (see Fig. 2) include diffuse gas–surface interaction at the wall boundaries (C, D, E), while in the open boundaries (A, B, F, G) the entering particles are defined by Maxwellian distributions according to the local pressure and temperature. Specular reflection is taken along the symmetry axis $r' = 0$ (H).

The governing equation and the associated boundary conditions are discretized in the molecular velocity space by a set of discrete molecular velocities and in the physical space by a second order finite volume scheme [9,10]. The resulting discretized equations are solved in an iterative manner. The numerical parameters provided in Table 1, ensure accuracy up to at least two significant figures in the numerical results.

Once the problem is solved the dimensionless flow rate is computed according to

$$W = 4\sqrt{\pi}\int_0^1 \rho(x,r)u_x(x,r)r\ dr \quad (3)$$

It is noted that the flow rate W is constant at each cross section along the tube. Then, the mass flow rate is given by $\dot{M} = W \times \dot{M}_{FM}$, where $\dot{M}_{FM} = R^2\sqrt{\pi}P_A/\upsilon_A$ is the mass flow rate through an orifice in the free molecular limit ($\delta_A = 0$). Benchmark computations in the free molecular regime for various tube lengths and pressure and temperature ratios have been performed and the results are in very good agreement (about 1–2%) with corresponding results obtained by expressions (5.7) and (5.9) in [4]. Other quantities of practical interest are the conductance and the throughput which are estimated as $C = \dot{M}R_g T_A/(P_A - P_B)$ and $Q = \dot{M}R_g T_A$ respectively.

4. Results and discussion

Numerical results for the dimensionless flow rates and the corresponding mass flow rates are presented in tabulated form

Please cite this article in press as: S. Pantazis, et al., Nonlinear vacuum gas flow through a short tube due to pressure and temperature gradients, Fusion Eng. Des. (2013), http://dx.doi.org/10.1016/j.fusengdes.2013.03.011

Table 2
Pressure driven flow through the tube.

Case	Ref. temperature, T_A (K)	Ref. pressure, P_A (Pa)	Pressure ratio, P_B/P_A	Ref. rarefaction parameter, δ_A	Dimensionless flow rate, W	Mass flow rate, $\dot{M}$ (kg/s)
I	300	0.3	0.2	2.16	4.38E−01	5.36E−06
	300	0.3	0.5	2.16	2.96E−01	3.62E−06
	300	0.03	0.2	0.216	3.48E−01	4.26E−07
	300	0.03	0.5	0.216	2.20E−01	2.69E−07
II	80	0.3	0.2	9.84	6.87E−01	1.63E−05
	80	0.3	0.5	9.84	5.48E−01	1.30E−05
	80	0.03	0.2	0.984	3.86E−01	9.15E−07
	80	0.03	0.5	0.984	2.51E−01	5.95E−07

Table 3
Temperature driven flow through the tube.

Case	Ref. temperature, T_A (K)	Ref. pressure, P_A (Pa)	Pressure ratio, P_B/P_A	Ref. rarefaction parameter, δ_A	Dimensionless flow rate, W	Mass flow rate, $\dot{M}$ (kg/s)
III	300	0.3	1.0	2.16	−1.28E−01	−1.57E−06
	300	0.03	1.0	0.216	−3.41E−01	−4.17E−07

Table 4
Pressure and temperature driven flow through the tube.

Case	Ref. temperature, T_A (K)	Ref. pressure, P_A (Pa)	Pressure ratio, P_B/P_A	Ref. rarefaction parameter, δ_A	Dimensionless flow rate, W	Mass flow rate, $\dot{M}$ (kg/s)
IV	300	0.3	0.2	2.16	5.66E−01	6.92E−06
	300	0.3	0.5	2.16	3.76E−01	4.60E−06
	300	0.03	0.2	0.216	3.00E−01	3.67E−07
	300	0.03	0.5	0.216	6.80E−02	8.32E−08

(Tables 2–4), while axial distributions of the bulk velocity are given in Fig. 3.

In Table 2, Cases I and II, corresponding to purely pressure driven flow are considered. The reference temperature is $T_A = T_B$ and thus no thermal creep flow is present. It is seen that for $P_A = 0.3$ Pa and a pressure ratio $P_B/P_A = 0.2$, when $T_A = 300$ K the mass flow rate is $\dot{M} = 5.36 \times 10^{-6}$ kg/s, while at $T_A = 80$ K the mass flow rate is increased up to $\dot{M} = 1.63 \times 10^{-5}$ kg/s. This is a significant increase of about 3.0 times. Furthermore by considering the corresponding cases of $P_B/P_A = 0.5$, although as expected the values of the mass flow rates are decreased, since the pressure difference leading the flow is smaller, again going from 300 K to 80 K, an increase of the mass flow rate from $\dot{M} = 3.62 \times 10^{-6}$ kg/s up to $\dot{M} = 1.30 \times 10^{-5}$ kg/s is observed, i.e. an increase of about 3.6 times. We remain in Table 2 and investigate the case of $P_A = 0.03$ Pa, i.e. having a gas rarefaction of about ten times less than before. By comparing the corresponding results it is seen that when the pressure ratio is $P_B/P_A = 0.2$ the flow rate is increased about 2.1 times (from 4.26×10^{-7} kg/s to 9.15×10^{-7} kg/s), while at $P_B/P_A = 0.5$ the increase is about 2.2 times (from 2.69×10^{-7} kg/s to 5.95×10^{-7} kg/s). These results clearly indicate the advantage of operating at low temperatures.

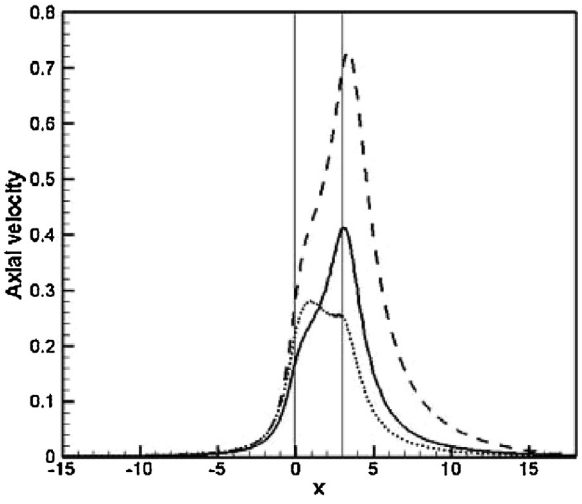

Fig. 3. Axial velocity along $r' = 0$ for pressure driven flow "Case I" at 300 K (solid line) and "Case II" 80 K (dashed line) as well as mixed flow "Case IV" (dotted line), with $P_A = 0.3$ Pa and $P_B/P_A = 0.2$.

In Table 3 the flow rates of Case III are tabulated. Now, the flow is driven only by a temperature gradient. In particular the wall temperature of the tube, as described in Section 2 is 300 K at $x' = 0$ mm and then it drops linearly at 80 K at $x' = 295$ mm, while from this point to the end of the tube $x' = 483$ mm remains constant. The negative signs in front of the flow rates indicate that the flow is in the opposite direction than the pressure driven flow discussed before. As expected, He flows from the low to the high temperature region. As the rarefaction parameter is decreased (i.e. the flow becomes more rarefied) the absolute value of W is increased. However, the corresponding mass flow rate is decreased and this is due to the fact that the mass flow rate in the free molecular limit $\dot{M}_{FM}$, used in the dimensionalization formula, is reduced directly proportional to the reference pressure (at $P_A = 0.3$ Pa and 0.03 Pa the values of $\dot{M}_{FM}$ are 1.22×10^{-5} kg/s and 1.22×10^{-6} kg/s respectively). It is noted that the computed thermal creep mass flow rates of 1.57×10^{-6} and 4.17×10^{-7} kg/s are not negligible compared to the corresponding mass flow rates in Table 2. Actually, in some cases particularly for the small pressure difference ($P_B/P_A = 0.5$) and for the more rarefied flow ($P_A = 0.03$ Pa) the results in absolute values are quite close. It is expected that the thermal creep flow will contribute significantly in the mixed flow to be studied next.

In Table 4 the flow rates of Case IV corresponding to the mixed pressure driven and the counter temperature driven flows are tabulated. In all cases the wall temperature of the tube varies from 300 K down to 80 K as described before in Section 2 (also in Case III). For the case of $P_A = 0.3$ Pa the computed mass flow rates of 6.92×10^{-6} kg/s and 4.60×10^{-6} kg/s are between the

Please cite this article in press as: S. Pantazis, et al., Nonlinear vacuum gas flow through a short tube due to pressure and temperature gradients, Fusion Eng. Des. (2013), http://dx.doi.org/10.1016/j.fusengdes.2013.03.011

corresponding ones for purely pressure driven flow at 300 K and 80 K. However, the gain is now significantly reduced. In particular for both pressure ratios the increase of the mass flow rate of operating in low temperatures compared to the mass flow rates at 300 K is only about 1.3 times larger. It is seen that the presence of the temperature driven flow in the opposite direction of the pressure driven flow results to a significantly reduced net mass flow rate. This reduction becomes even more dominant in the case of reference pressure $P_A = 0.03$ Pa. As it is seen in Table 4, in this case the computed mass flow rates of 3.67×10^{-7} kg/s and 8.32×10^{-8} kg/s are even smaller than the corresponding ones in Table 1 at 300 K and as a result there is no gain at all working at low temperatures. This is well justified by the fact that the mass flow rate in the pressure driven flow is reduced as the flow becomes more rarefied.

Next, some insight in the flow characteristics is provided by plotting the x-component of the bulk velocity along the symmetry axis ($r' = 0$). In Fig. 3 the axial velocities for the pressure driven flow (Cases I and II) at 300 K and 80 K as well as for the combined pressure and temperature driven flow (Case IV) are presented for the reference pressure of $P_A = 0.3$ Pa and pressure ratio $P_B/P_A = 0.2$. Comparing the magnitude of the velocities for the two flows at 300 K and 80 K of Cases I and II it is seen that the former one is always smaller. The flow at 80 K is much faster resulting to a larger mass flow rate. Also, the magnitude of the velocity of Case IV is, in general, smaller than the ones of Cases I and II. All these observations are in agreement with the tabulated mass flow rates in Tables 2 and 4. In addition, the results for Case I are in qualitative agreement with the ones in [11].

5. Concluding remarks

The flow of a rarefied gas through a tube due to both pressure and temperature gradients has been investigated based on a kinetic approach. Results are presented for specific geometric and flow parameters in the transition regime with the objective of investigating performance optimization for a cryo-mechanical pump, which is under development at CEA-Grenoble.

Based on the obtained results it may be pointed out that for the cases investigated here the presence of the counter temperature driven flow significantly reduces the net flow. Also, the concept of operating the pump in low temperatures is more advantageous when the flow is not very rarefied driven by large pressure differences. In addition, it will be interesting to optimize the design of the heat exchanger part of the pump in order to reduce the effect of the thermal creep flow.

Acknowledgments

Part of this work has been supported by the Association EURATOM/Hellenic Republic and by the EFDA/GOT programme VACU-TEC. The views and opinions expressed herein do not necessarily reflect those of the European Commission.

References

[1] J. André, F. Millet, J.P. Périn, P. Saint-Bonnet, SOFT2012.
[2] N. Hadacek, J.P. Périn, F. Viargues, Vacuum 60 (2001) 85.
[3] F. Sharipov, Journal of Vacuum Science and Technology A 14 (1996) 2627.
[4] F. Sharipov, V. Seleznev, Journal of Physical and Chemical Reference Data 27 (1998) 657.
[5] F. Sharipov, Journal of Vacuum Science and Technology A 15 (1997) 2434.
[6] K. Ritos, J. Lihnaropoulos, S. Naris, D. Valougeorgis, Heat Transfer Engineering 32 (2011) 1101.
[7] A.A. Alexeenko, S.F. Gimelshein, E.P. Muntz, A. Ketsdever, International Journal of Thermal Sciences 45 (2006) 1045.
[8] E.M. Shakhov, Fluid Dynamics 3 (1968) 95.
[9] S. Pantazis, Ph.D. Thesis, University of Thessaly, 2011.
[10] S. Misdanitis, S. Pantazis, D. Valougeorgis, Vacuum 86 (2012) 1701.
[11] S. Varoutis, D. Valougeorgis, F. Sharipov, Journal of Vacuum Science and Technology A 27 (2009) 1377.

Please cite this article in press as: S. Pantazis, et al., Nonlinear vacuum gas flow through a short tube due to pressure and temperature gradients, Fusion Eng. Des. (2013), http://dx.doi.org/10.1016/j.fusengdes.2013.03.011